

## Use of Imaging for Nuclear Material Control and Accountability

James A. Mullens, Paul A. Hausladen, Philip Bingham,  
Daniel E Archer, Brandon Grogan, John T Mihalcz

Oak Ridge National Laboratory

### **Abstract**

The recent addition of imaging to the Nuclear Materials and Identification System (NMIS) using a small portable DT neutron generator with an embedded alpha detector to time and directionally tag neutrons from the DT reaction is discussed. The generator weighs ~35 lbs including power supplies ( $5 \times 10^7$  n/sec) and operates on 50 watts power. Thus, the source can be easily moved to a variety of locations within an operational facility with minimum impact on operations or can be used at a fixed location for example to monitor receipts. Imaging NMIS (INMIS) not only characterizes the detailed shape of a containerized object by transmission tomography but determines the presence of fissile material by measuring the emitted radiation from induced fission. Previous work has shown that this type of imaging has a variety of applications other than nuclear material control and accountability (NMC&A). These include nonproliferation applications such as verification of configuration of nuclear weapons/components shipped or received, warhead authentication behind an information barrier, and traceability of weapons components both fissile and non fissile in dismantlement and counter terrorism. This paper concentrates on the use for NMC&A. Some of the NMC&A applications discussed are: verifying inventory and receipts, making more accurate holdup measurements especially where thicknesses of materials affect gamma ray spectrometry, determining the shape of unknown configurations of fissile materials where the material type may be known but not the form, determining the oxidation of fissile metal in storage cans, fingerprinting the content of storage containers going into a storage facility, and determining unknown configurations for criticality safety,

### **Introduction**

Tomographic and radiographic imaging capabilities have been added to the Nuclear Materials Identification System (NMIS) [ref 1] at Oak Ridge National Laboratory (ORNL). The system uses transmission imaging with a time and directionally tagged portable DT generator [ref 2] or a time tagged Cf spontaneous fission source [ref 3]. Neutrons from the DT generator are more penetrating of hydrogenous materials than Cf fission neutrons by a factor of ~5. However Cf is adequate for objects with low attenuation and where measurement time is not a factor. The generator has an additional advantage in that it can be turned off when not in use. These imaging capabilities supplement the system's existing time-correlation (coincidence) measurements to quantify fissile material and enhance the system's ability to identify fissile material in containers. This capability has a variety of application in NMC&A such as determination of the fissile mass holdup in pipes, especially in situations where heavy deposits produce self shielding that make gamma ray spectrometry determinations of hold up have large uncertainties. One such holdup measurement was satisfactorily performed in 1998 at the so called "hockey stick" deposit at the K-29 building of the former gaseous diffusion plant at Oak Ridge (Ref 3). The present NMIS with imaging can satisfy all DOE

requirements for confirmation of receipt of weapons components at Y-12, and its continued development will lead to a system that accurately measures the fissile mass in Y-12 receipts. Other than identification and confirmation of weapons components there are a variety of other applications such as: determining the form of legacy materials such as HEU in storage cans where the form is not known, fingerprinting the configurations of HEU going into long term storage facilities, determining the fissile mass in plant components that process oxide and other materials without cleaning out the components, comparing the images of fissile materials in shipping containers where the detailed shape is available from the shipper, determining the amount of oxidized metal in storage cans for fissile metal, determining unknown configurations of fissile materials for criticality safety, and identifying appropriate standards for other NMC&A measurements on cans where internal configuration is not known, etc. The present status of this system is described in this paper and examples of imaging of objects with both a DT generator and a Cf source are presented.

## METHODOLOGY

Fig. 1 shows a plot of the time distribution of counts after the DT reaction. Three regions are of interest. In region 1, the gamma rays from induced fission and inelastic neutron scattering are detected first because they travel to the detectors with the speed of light and arrive before the transmitted neutrons. In region 2, the 14.1 MeV transmitted neutrons arrive at the detector. Region 2 also contains forward elastically scattered neutrons that have little change in direction and energy for highly enriched uranium (HEU). Finally, in region 3 the neutrons and gamma rays from induced fission in the HEU are detected and arrive with an amplitude and time dependence characteristic of the HEU mass and multiplication. Region 2 is used for the imaging measurements, while region 3 is used to distinguish HEU from depleted uranium (DU).

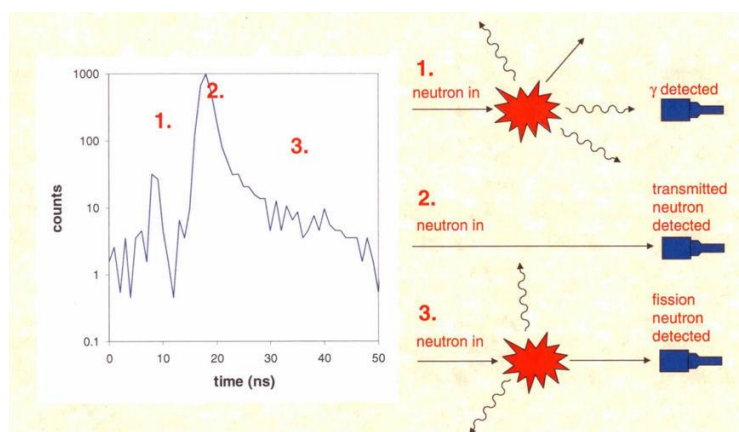


**Fig. 1. Typical time distribution of counts in a plastic scintillator after the DT reaction in a transmission measurement through a highly enriched uranium metal.**

The imaging measurement with a DT generator consists of measuring the detector counts as a function of time after the DT reaction with the sample between the source and the detectors  $I(t)$  and the count rate as a function of time without the sample present  $I_0(t)$

using the relationship  $I(t) = I_0(t)exp(-\mu x)$ , where  $x$  is the sample thickness, and  $\mu$  is the attenuation coefficient to obtain the value of  $\mu x$ , the attenuation. The values of  $I$  and  $I_0$  are obtained by integration of the transmission peak shown in region 2 of Fig. 1 with an empirical correction to remove some scattering. This imaging was performed as a function of height using a scanner that could rotate the eight small  $1 \times 1 \times 6$ -in.-thick detectors  $15^\circ$  in the horizontal plane to simulate a larger number of detector positions.

The time distribution of counts in 4 plastic scintillators spaced  $\sim 100$  cm from the source for a time tagged Cf spontaneous fission source is shown in Fig. 2. The initial peak at the time of flight of gamma rays ( $\sim 3$  nanoseconds) from the source fission to the detector is the prompt gamma rays and is broadened by the time resolution of the detection systems for detecting spontaneous fission in the time tagged source and the event in the detector. The following peak (25-80 nanoseconds) is the neutron distribution whose time dispersion is determined by the energy distribution of prompt neutron emitted in spontaneous fission of Cf. Beyond 80 nsec, the distribution is mainly from neutron scattering from the floor. Separation of the gamma rays and neutrons allows both neutron and gamma ray imaging, with neutrons sensitive to light materials and gamma rays sensitive to heavy materials. For neutron imaging the area near the peak of the neutron distribution was used while for gamma rays the integral of the gamma peak was used.

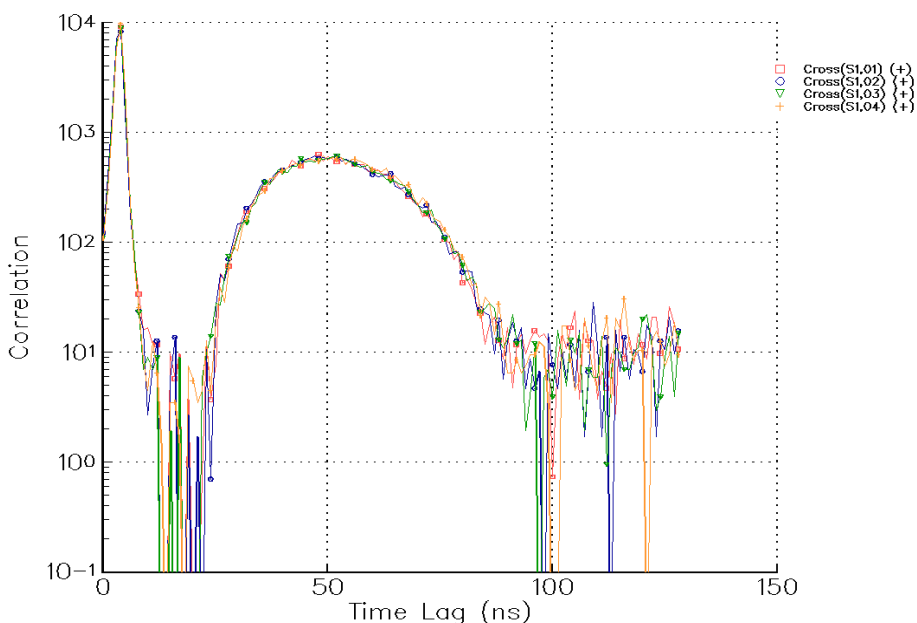


**Fig. 2 Typical time distribution of counts from a detector after spontaneous fission of Cf. Initial peak is from gammas and subsequent peak is from the neutron distribution.**

The source of preference is the DT generator with embedded alpha detector because of the penetrating capability of 14 MeV neutrons, the shorter measurement time, and the ability to turn it off when not in use.

### RESULTS FOR DU METAL CASTING WITH DT GENERATOR

A standard DU-metal annular Y-12 National Security Complex storage casting in a steel can was available for imaging measurements at ORNL. This casting has an outside diameter of 12.70 cm, an inside diameter of 8.89 cm, and a height of approximately 14 cm, with a density of approximately  $18.8 \text{ g/cm}^3$ . The casting was inside a 0.05-cm.-thick sealed steel can with an outside dimension of 15.2 cm and a height of 22.9 cm. A photograph of the imaging measurement for the casting on a rotational platform is shown in Fig. 3, with the DT generator on the left and the eight  $1 \times 1 \times 6$ -in.-thick plastic scintillation detectors on the right [4].

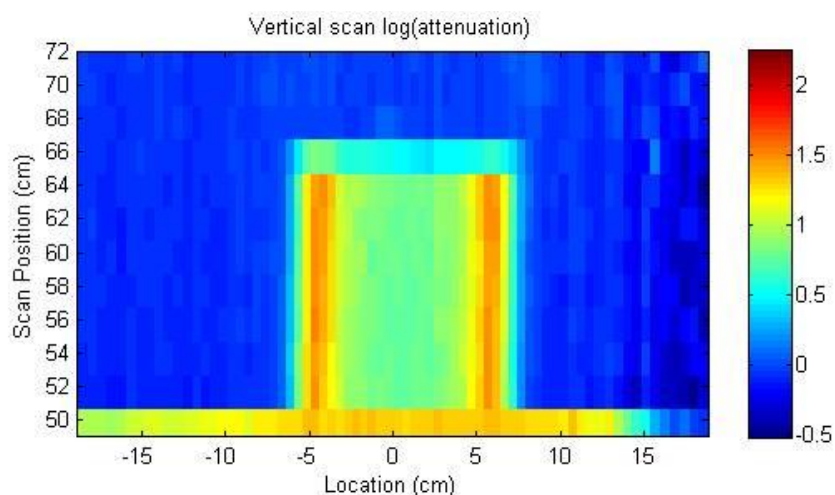


**Fig. 3. Source-uranium metal-casting-detector configuration for imaging.**

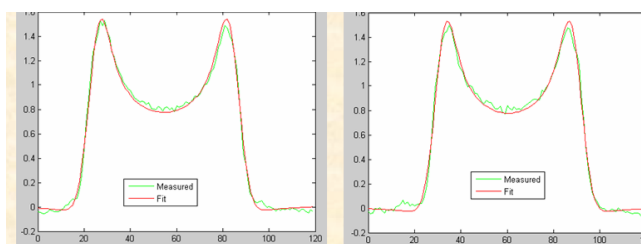
Initially a vertical scan was performed over the full height of the casting, and the results are shown in Fig 4. A full vertical scan at a single projection angle provides an overall picture of the object to be imaged and allows the user to choose a particular height to image further. While the scan shown in Fig 4 was obtained with high resolution at each level, these vertical scans can often be taken much quicker with fewer pixels and shorter exposures without affecting the ability to locate an area of interest. Vertical scans can be interpreted in the same fashion as x-ray images. The DU casting on top of the rotational platform can clearly be seen in the image. Next, two high-resolution scans were made at one height through the casting. These projections were captured at two rotational positions  $90^\circ$  apart. For both positions of the rotational platform, the 1-in.-square detectors were shifted  $1/3$ -in. for successive measurements until the imaging arc was fully covered. Measuring with finer detail than the 1-in. detector face yields some gain in image resolution, depending in part on the image reconstruction method used.

Fig. 5 shows the attenuation values for each of these positions in both projections ( $0^\circ$  and  $270^\circ$  rotational positions). For a cylindrically symmetric casting, this  $90^\circ$  rotation will confirm symmetry and determine the position of the casting with respect to the center of

rotation. For objects that are not cylindrically symmetrical about the axis of rotation, more projections are required to obtain the shape of the contents of the can. The NMIS analysis software includes a model-based fitting algorithm to determine geometric dimensions and attenuation coefficient values. This algorithm begins with the user entering an initial geometry of basic shapes from data such as that shown in Fig. 4 and selecting key parameters (positions, sizes, and attenuation coefficients), allowed to vary during the fit. The fit uses an unconstrained nonlinear optimization algorithm in conjunction with a simulation tool based on ray tracing to find a fit of the measured projections to those generated by simulating the geometry. The results of fitting the attenuation projections at  $0^\circ$  and  $90^\circ$  rotational positions are shown in Fig. 4, and the dimensions obtained are given in Table 1.



**Fig. 4.** Full scan of DU casting: lag of attenuation versus lateral location and height above the floor.



**Fig. 5.** Attenuation projections at  $0^\circ$  and  $90^\circ$  rotational positions and the results of fitting the data.

**Table 1. Dimensions in centimeters from fit of casting data set containing two projections 90° apart.**

Parameter	Initial guess	Final fit	Actual dimensions
Inner diameter (cm)	10.00	8.56	8.89
Outer diameter (cm)	11.00	12.93	12.81
Attenuation coefficient (2/cm or cm <sup>-1</sup> )	0.280	0.202	0.280
X offset (cm)	0.00	-0.418	Unknown
Y offset (cm)	0.00	0.570	Unknown

The fitted dimensions are close to the actual. These measurements are with 1- by 1-in. pixels (detectors). Reduced pixel size would improve the accuracy of the dimensions. The fitted attenuation coefficient (0.202 cm<sup>-1</sup>) is lower than the actual (0.28 cm<sup>-1</sup>) because neutrons scattered at small angles from uranium still arrive at the detector and at nearly the same time as the directly transmitted neutrons. With proper correction for scattering, the values of the attenuation coefficients can be fixed for known materials, and more accurate dimensions can be obtained. Based on the X offset in Table 1, the axis of the casting was approximately 0.42 cm farther from the detector array than the axis of rotation. A second set of experiments were performed on the DU casting by placing shielding around the casting. Two different shielding configurations were measured: (1) a 1-in.-thick lead box surrounding the steel can and (2) a 1-in.-thick lead box plus 4-in.-thick lead plates and bricks added to the front and back as shown in Fig. 6.



**Fig. 6. DU casting with 1-in.-thick lead box surrounding and 4-in. thickness of lead plates in front and back.**

In an effort to determine whether the internal components still provide a useful signature, a second set of projections was obtained for just the shielding without the DU casting and used to normalize the projections ( $I_0$ ). The measurement times for the bare casting and the casting with 2 in of lead were 2 minutes and that for the casting with 10 in of lead was 10 minutes. The images for the different configurations of lead shielding are shown in Fig. 7. Based on these results, the casting is still distinguishable with 5-in.-thick lead shielding front and back. Thus, the transmission was measured through 10 in. of lead and the casting. This result illustrates that if the shielding or container material is known and available, a measurement of transmission,  $I_0$ , with the shielding or container in place can normalize out the container and shielding effects.

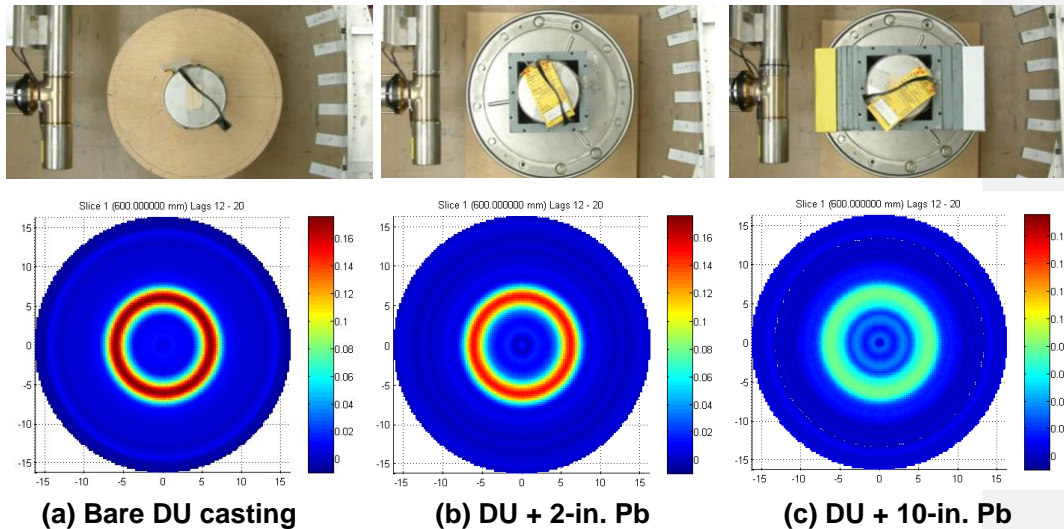
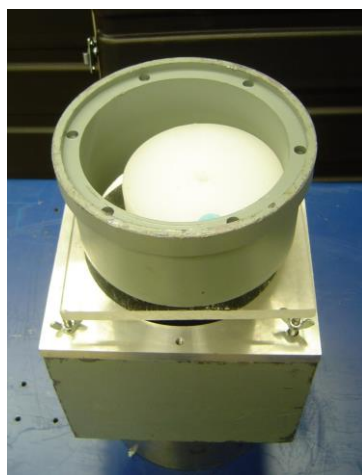


Fig. 7. Various shielded casting configurations and resulting images.

#### MEASUREMENT OF A 3D OBJECT WITH CF

Imaging measurements were performed for a variety of objects that were not cylindrically symmetric. In this case the object needs to be rotated to measure the projection at various angles. One such object located is shown in Fig. 8. The bottom of this object consists of a 8-in-square lead with a 6.5-in.-diam. central hole that is 6.75 in high. Spaced 0.5 in above that is a 0.5-in-thick, 7-in-square piece of Plexiglas. On the Plexiglas is a 3.5-in-high, 6.5-in-OD, 5.5 -in -ID lead part whose outside diameter increases to 7 in. for the top 0.75 in. Inside the top piece of lead and resting on the Plexiglas is a 3.5-in.-diam., 2-in.-high polyethylene cylinder adjacent to the inside surface of the lead. These features of the object are visible in Fig. 8. This was a contrived test object used for training to test the ability to image an unknown 3D object. The object was then inserted into a drum and located as in Fig. 9 between the Cf source (on the left) and 16 plastic scintillators (on the right) on a radial arm that could be rotated. The object was raised off the bottom of the drum by a low mass metal ring and plate.



**Fig. 8. 3D object of lead, aluminum, polyethylene, and Plexiglas.**

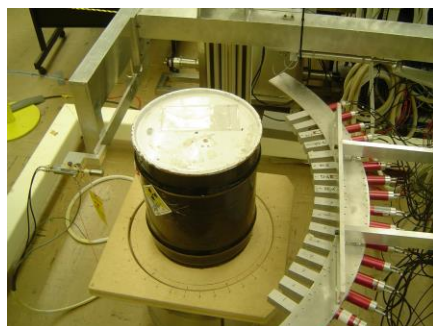


**Fig. 9. 3D test object in a container on the rotating table  
between the Cf source and the detectors.**

The initial measurements were a vertical scan of the object in the container with the arm supporting the detectors rotating laterally to simulate other radial detector positions. The results of these measurements are shown in Fig. 10 and 11 where 2 dimensional plots of the attenuation length are presented. In the neutron scan the polyethylene and the Plexiglas are clearly visible whereas they are not in the gamma scan. This is not the case when imaging with a DT generator which is sensitive to both light and heavy materials [ref].

Based on these vertical scans, a detailed image was measured at 2 vertical locations through the middle of the lower lead and through the middle of the polyethylene. Since these objects were not cylindrically symmetric, the transmission was measured at 18 different projection angles. The reconstructed images are shown in Figs. 12 and 13. Clearly the configurations of the test object at the 2 heights are determined. Future work

**Comment [JAM1]:** Add reference.

in imaging testing on 3D objects will employ an automated object turntable. The use of a DT generator with pixilated alpha detector for this type of measurement will facilitate much better imaging through removal of scattering in a shorter measurement time.

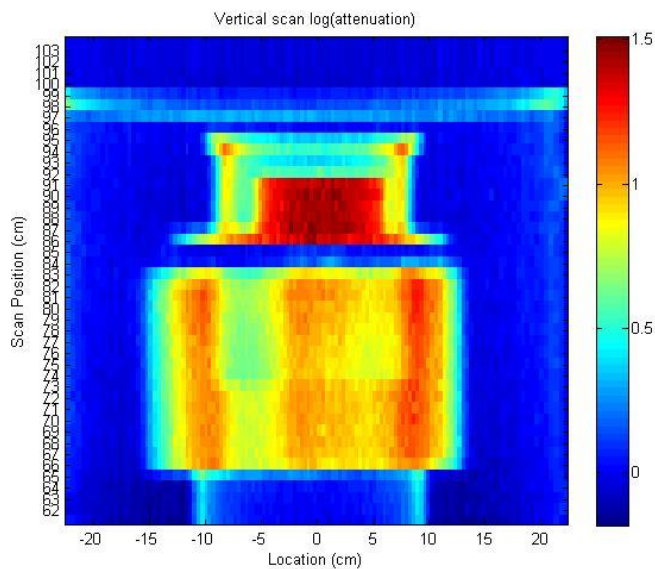
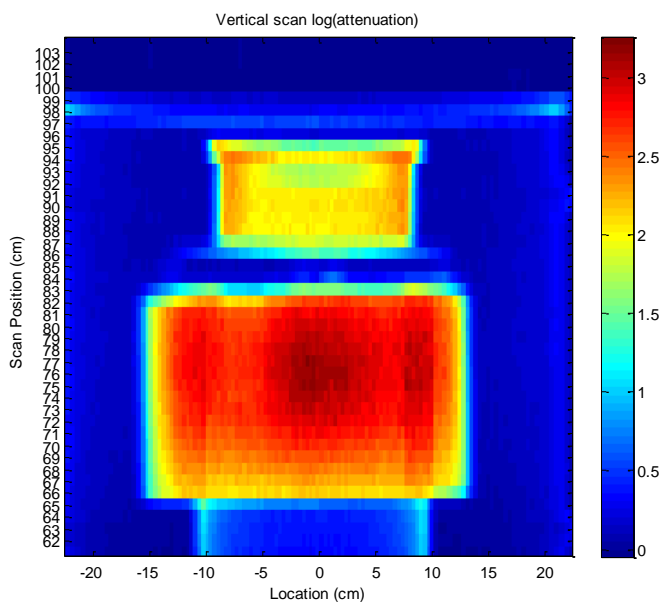
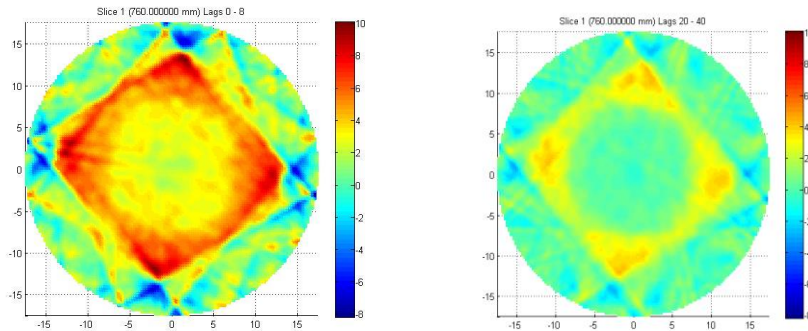


Fig. 10. Neutron radiograph of the test object from the vertical scan.



**Fig.11. Gamma radiograph of the test object from the vertical scan.**



**Fig 12. Gamma and neutron images of the test object through the lower lead.**

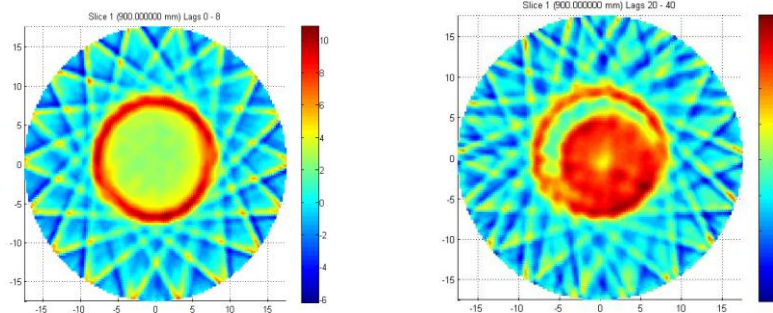


**Fig. 13. Gamma and neutron images through the test object at the height of the polyethylene.**

## APPLICATIONS

The imaging capability of NMIS can enhance NMC&A:

1. Determination of the configuration of items in containers, and it is ideal for fissile material transfers between facilities. This capability is accomplished by providing the detailed configuration of the fissile and non-fissile components of an item under scrutiny. The images can be compared to drawings provided by the shipper avoiding repackaging delays to verify the contents of a shipment that will not be immediately used. Induced fission emitted radiation can be evaluated to distinguish fissile from non fissile materials.
2. Periodic inventory confirmation.
3. Determination of the form of legacy materials such as HEU in storage cans where the form is not known.
4. Determination of unknown configurations of fissile materials for criticality safety and identification or to determine appropriate standards for other NMC&A measurements.

5. Determination of the amount of oxidation of fissile metal in cans.
6. Providing more accurate hold up measurements in pipes and process applications where the material and shape are known and process vessels can not be emptied. In some cases the density distribution in the container can be measured accurately so that the mass can be inferred to a few percent

## CONCLUSIONS

The imaging capability of NMIS using a DT generator with an embedded alpha detector can enhance NMC&A for a wide variety of NMC&A applications addressing such problems as fissile transfers, fissile inventory, unknown fissile configurations, oxidation of fissile metal, and hold up in pipes and process vessels. This type of imaging has a variety of other uses such as verification of the configuration of nuclear weapons/components shipped or received, warhead authentication behind an information barrier, traceability of both fissile and non-fissile weapons components/parts during dismantlement, and counter terrorism.

## REFERENCES

1. J. T. Mihalcz, J. A. Mullens, J. K. Mattingly, T. E. Valentine, "Physical description of nuclear materials identification system (NMIS) signatures," *Nucl. Inst. and Meth. A* **450** (2000): 531.
2. J. A. Mullens, "Addition of Tomographic Capabilities to NMIS", Y/LB-16,160, March 2003, <http://www1.y12.doe.gov/search/library/documents/pdf/YLB-16160.pdf>.
3. Wyatt, M.S., et al. 1998. "Characterization of an Enriched Uranyl Fluoride Deposit in a Valve and Pipe Intersection Using Time-of-Flight Transmission Measurements with  $^{252}\text{Cf}$ ," *Proc. Inst. of Nuclear Materials Management Meeting, Naples, FL, July 26–30, 1998*.
4. "API120 D-T Neutron Generator User Manual," Thermo Electron Corporation, 5074 List Drive, Colorado Springs, CO 80919, [www.thermo.com/neutrongenerators](http://www.thermo.com/neutrongenerators).